Quaternary Geochronology 83 (2024) 101592

Contents lists available at ScienceDirect

Quaternary Geochronology

journal homepage: www.elsevier.com/locate/quageo

Research paper

Absolute dating of sediments forming the Lena river terraces (Northeastern Siberia)

Anzhela N. Vasilieva [a,*], Andrew S. Murray [b], Natalia A. Taratunina [c], Jan-Pieter Buylaert [c], Vasiliy M. Lytkin [d], Grigoriy I. Shaposhnikov [d], Thomas Stevens [e,f], Gábor Ujvari [g,h], Titanilla G. Kertész [i], Redzhep N. Kurbanov [j]

[a] *Al-Farabi Kazakh National University, Almaty, Kazakhstan*
[b] *Department of Geoscience, Aarhus University, Aarhus, Denmark*
[c] *Department of Physics, Technical University of Denmark, Roskilde, Denmark*
[d] *Institute of Geography and Water Security, Almaty, Kazakhstan*
[e] *Department Earth Sciences, Uppsala University, Uppsala, Sweden*
[f] *Department of Geosciences and Geography, University of Helsinki, Helsinki, Finland*
[g] *Institute for Geological and Geochemical Research, HUN-REN Research Centre for Astronomy and Earth Sciences, Budapest, Hungary*
[h] *CSFK, MTA Centre of Excellence, Budapest, Hungary*
[i] *Isotope Climatology and Environmental Research Centre, Institute for Nuclear Research, H-4026 Debrecen, Bem tér 18/c, Hungary*
[j] *Institute of Water Problems, Hydropower and Ecology, National Academy of Science of Tajikistan, Dushanbe, Tajikistan*

ARTICLE INFO

Keywords:
Fluvial terraces
Aeolian deposits
Quaternary
Late pleistocene
Holocene
Aeolian dunes

ABSTRACT

Sediments of the Lena River represent an important environmental archive for understanding the Quaternary history of North-Eastern Siberia. However, at present, the structure, origin and age of the Lena River terraces are poorly known. This article presents results of lithofacies analysis and absolute dating of the Ust'-Buotama section exposing the fourth (Bestyakh) terrace of the Lena River. We report the first quartz and K-feldspar luminescence ages, the reliability of which was argued by age relations and standard tests. Three stratigraphic units have been recognized in the section (depths from the top): lacustrine-alluvial deposits (85–120 m) of the Mavrinka Formation; aeolian sand deposits of the Dolkuma Formation (23–85 m), and Holocene aeolian dune sediments (0–23 m). The resulting chronology suggests that the sediments of the Mavrinka Formation were deposited no later than 300 ka (MIS 9 or later). Deposition of the Dolkuma Formation occurred from ~30 ka to ~15 ka (late MIS 3 - late MIS 2). Holocene aeolian dune formed during initial Neoglacial cooling post climatic optimum (c. 5.5 cal ka BP). More extensive Late Holocene dune sediments which formed ~400 years ago are coeval with Little Ice Age (11th-19th centuries).

1. Introduction

North-Eastern Siberia is a vast, geographically diverse region whose palaeoenvironmental history remains poorly understood. Despite many decades of research, our understanding of past environmental changes in the region is limited; this lack of knowledge includes the glacial history of the Verkhoyansk and Chersky mountain ranges, the sedimentary evolution of the wide Yakutian plains, as well as the role of permafrost in the regional Pleistocene landscape evolution and depositional environments. The Lena River is a very important feature of the region, and it has played a crucial role in landscape-building processes throughout the Quaternary period. The Lena River is one of the largest rivers of Eurasia, draining much of eastern Siberia, and its sediments provide a record of former climatic, tectonic and geomorphic conditions. As such, the complex geologic/geomorphic evolution of the Lena River valley has been the focus of considerable attention due to its significance in understanding the Quaternary history of the North-Eastern Siberia.

The number, age and origin of the Lena River terraces have been debated for over 50 years. Geomorphological mapping of the Central Yakutian Plain was first undertaken by Zolnikov and Popova (1957) they subdivided the region into three geomorphological zones: 1) an ancient, highly dissected erosional plain; 2) an alluvial plain of

* Corresponding author.
E-mail address: angievasilieva@gmail.com (A.N. Vasilieva).

https://doi.org/10.1016/j.quageo.2024.101592
Received 15 November 2023; Received in revised form 5 July 2024; Accepted 5 July 2024
Available online 14 July 2024

Quaternary age, and 3) the modern river valley. Soloviev (1959) recognized a stair of eleven terraces grouped into three levels (elevation above the modern channel): 1) low accumulative terraces: the floodplain (up to 8–10 m), Yakutsk (14–17 m) and Sergelyakh (18–22 m) terraces; 2) intermediate cut-and-fill terraces: Kerdem (26–36 m), Bestyakh (56–78 m), Tyungulu pseudoterrace (66–98 m), Abalakh (116–134 m), and Magan (156–176 m); 3) elevated erosional terraces: Emilsk (194–212 m), Kirensk (250–270 m), and Verkholensk (300–325 m). Soloviev (1959) also suggested that these terraces represented three different landforms: normal fluvial terraces, alluvial plains, and erosional plains. By contrast, Korzhuev (1977) identified eight terraces of different ages from 3 to 200 m above the modern channel. Furthermore, Katasonov and Ivanov (1973) presented detailed descriptions of several key Pleistocene exposures in the middle Lena River. Later, Ivanov (1984) recognized the floodplain, five terraces (elevation above the modern channel): Yakutsk (8–10 m), Sergelyakh (12–14 m), Kerdem (15–25 m), Bestyakh (45–75 m), Tyungulu (65–100 m) and the Abalakh erosional-depositional plain (115–135 m).

On top of all this previous work, a more recent study by (Spektor and Spektor, 2002) further revised the geomorphological structure of the Lena River valley, combining the Sergelyakh and Yakutsk terraces of Soloviev (1959) ievinto one level and adding the Dolkuma terraced level between the Kerdem and Bestyakh terraces. However, morphometric studies by Pravkin et al. (2018) did not support the levels recognized in the early classical works and found no clear boundaries between the Tyungulu, Bestyakh and Kerdem terraces. These authors came to the radically different conclusion that these terraces were relatively young, and that the entire surface of the Lena River valley had a similar geomorphic history, in contrast to the adjoining piedmonts and the Lena Plateau.

Ivanov (1984) attributed the significant decrease in elevation of the Bestyakh and Kerdem terraces between the mouths of the Buotama and Aldan Rivers to tectonic subsidence of the base of Quaternary sediments towards the north. Galanin (2021) came to the same conclusion, noting that the maximum elevation of the Bestyakh Terrace (90–120 m above the modern channel), as well as the maximum thickness of the Dolkuma Formation sands (70–80 m) are observed in the Ust'-Buotama outcrop 120 km south of Yakutsk. The elevation of the terrace decreases northwards to 40–60 m above the modern channel near Nizhny Bestyakh, and to 25 m above the modern channel (Kerdem Terrace) at the Peschanaya Gora outcrop 100 km further north. Along the 60-km section to the mouth of the Aldan River, the surface reduces to 12–18 m above the modern channel comprising the first terrace above the floodplain (Galanin, 2021).

While much previous work assumed that terraces levels were controlled by typical cyclic accumulative river terraces topped by floodplain facies deposited at the end of each sedimentation cycle, recent data has cast doubt on this. Galanin (2021) argues that the modern relief was rather formed by polygenetic gradational surfaces (erosional-depositional plains), the relative height and topographic features of which are not associated with the cyclic cutting of the Lena River, but with subaerial (aeolian) sedimentation and deflation during the Middle and Late Pleistocene (Galanin, 2021); this argument is based on the observation that the terraces of different heights have similar structures in e.g. the basement and surface. Both the Kerdem (18–25 m above the modern channel) and Bestyakh (90–120 m above the modern channel) terraces consist of alluvial pebbles of the Middle Pleistocene Bestyakh Formation at their base (at the level of the modern Lena River channel), while the upper parts of both terraces are composed of cross-bedded sands of the Dolkuma Formation, accumulated during MIS 2 and before the Holocene (Kamaletdinov and Minuk, 1991). In Central Yakutia, the Bestyakh and Kerdem terraces contain three main formations (Bestyakh, Mavrinka and Dolkuma) of varying thicknesses. A common feature of these terraces is that their surface is covered with several generations of stabilized parabolic and spear-shaped dunes composed of cross-bedded quartz sands up to 10–15 m in thickness. Occasional active (unvegetated) dunes such as the modern Lena Dune can be up to 30 m in thickness. Saamys-Kumaga, the largest active dune field located in the southern part of the Bestyakh Terrace, is about 80 m above the modern channel, 1 km wide and 3 km long (Galanin, 2021). Currently, active dunes cover about 3000 km^2 in Central Yakutia. By contrast, the high terraces of the Lena River (the Tyungulu and Tabaga terraces and the Abalakh plain) have a different structure. Unlike the Bestyakh and Kerdem terraces, their surface is mantled by 10–60 m of thin-bedded silts, increasing in thickness from the valley thalweg towards the upland summits. No consensus exists concerning the origin of these cover deposits.

Initially, the preliminary age of the terraces was determined by morphometric characteristics, palaeomagnetic data and findings of mammalian fauna. Thus, based on the findings of *Priscus longicornis* (Grom) and the *early type Mammuthus primigenius* (Blum) in the deposits, the Abalakh Plain, 115–135 m above the modern channel, was formed during the Middle Pleistocene (Lungersgauzen, 1957; Soloviev, 1959; Rusanov, 1968). In1973, E.M. Katasonov and M.S. Ivanov first obtained thermoluminescence ages of 300 ka and 176 ka for the alluvial part of the Mammoth Gora outcrop of the Abalakh Plain. Pravkin et al. (2018) for the “Edeitsy” outcrop got 2 IR ages – 234 ka and 182 ka. Waters et al. (1997a, 1999) obtained 9 thermoluminescence ages for the site Diring Yuryakh located on the Tabaga Terrace – 366-240 ka and 17-13 ka. Here, Lukyanycheva et al. (2024) obtained 10 OSL ages for the upper part of aeolian deposits – 21-9 ka. The age of the fifth (Tyungulu) terrace alluvium on the geological map dates to the Middle Pleistocene (Geology of the USSR, 1979; Ivanov, 1984). The fourth (Bestyakh) terrace consists of four different stratigraphic units of sediments (bottom-up): 1) based on the findings of *Bison Priscus longicornis* (Grom)*, Mammuthus primigenius* (Blum), the basal alluvium of the Bestyakh formation was formed during the Tobolsk time of the Middle Pleistocene MIS 11-MIS 9 (Lungersgauzen, 1961; Alekseev, 1978; Ivanov, 1984). There are currently no absolute ages of the formation. 2) lacustrine-alluvial deposits of the Mavrinka formation, based on findings of mammoth fauna (*Mammuthus* sp., *Coelodonta antiquitatis Blum.*, *Bison priscus Boj.*, *Ovis nivicola Esch.*, *Rangifer tarandus* L), date from the second half of the Middle – early Late Pleistocene MIS 7-MIS 5 (Alekseev et al., 1990; Kamaletdinov and Minuk, 1991); 3) aeolian sand of Dolkuma formation, which accumulated at the end of MIS 3-MIS 2 (Kamaletdinov and Minuk, 1991; Grinenko et al., 1995; Pravkin et al., 2018; Galanin et al., 2018; Galanin and Pavlova, 2019; Galanin, 2021); 4) modern Holocene dune that accumulated in MIS 1 (Galanin et al., 2018; Galanin and Pavlova, 2019; Galanin, 2021). Nine radiocarbon ages (22-8 ka) were obtained for the cover sands of the third (Kerdem) terrace, which indicate that the formation of the terrace was completed at the end of MIS 2-at the beginning of MIS 1 (Ivanov, 1984; Alekseev et al., 1984, 1990; Kamaletdinov and Minuk, 1991; Galanin, 2021). The accumulation of sands in the lower part of the second (Sergelyakh) terrace occurred 19-17 ka (Ivanov, 1984; Grinenko et al., 1995; Pravkin et al., 2018). According to radiocarbon ages (Grinenko et al., 1995; Pravkin et al., 2018), the floodplain is hundreds of radiocarbon years old, and the first (Yakutsk) terrace is 10 ka.

It can be seen from the above that the structure, genesis and age of the main landforms in the Lena River valley are still debated. There is a considerable divergence of views in the literature regarding the number, genesis, structure and correlation of terraces, and thus there is a pressing need for detailed sedimentological and stratigraphic studies, and for absolute dating (Galanin, 2021). In an attempt to find answers to some of these controversial questions, we have undertaken a study to characterize the structure of Quaternary sediments in the Lena River valley, and to constrain their age using optically stimulated luminescence (OSL). This article presents the results for the Ust'-Buotama outcrop, one of the most important and well-known sections in the middle Lena River.

2. Study area and previous interpretations of the Ust'-Buotama outcrop

The Ust'-Buotama outcrop (61.232091 °N., 128.602046 °E) is located on the right bank of the Lena River, 130 km upstream from the city of Yakutsk. This section provides an excellent exposure of the Bestyakh Terrace, the most distinctive accumulation terrace along the Lena River (Fig. 1). The outcrop has a maximum height of about 120 m above the modern channel, including an active aeolian surface, and a length of over 2.5 km. The Bestyakh terrace itself extends over a 300-km stretch of the Lena River valley, from the Lena Pillars to the mouth of the Aldan River (Fig. 1). In this segment, the river runs through two geomorphological areas, Buotoma-Sinsk and Pre-Yakutsk, which differ in valley morphology, as well as in the parameters and composition of terrace sediments (Kamaletdinov and Minuk, 1991).

Within the Buotoma-Sinsk geomorphological area, the 30–40 km wide Lena River valley is incised into Cambrian carbonate rocks. The Bestyakh Terrace in this area can be traced from the confluence of the Echite River to the confluence of the Buotama River, with heights of between 90 and 120 m above the modern channel and a maximum width of 3 km. The terrace adjoins the Late Pliocene and Gelasian-Calabria high terraces (Kamaletdinov and Minuk, 1991), and it contains deposits of the Bestyakh, Mavrinka, Dolkuma formations and Holocene deposits; we studied these formations in detail in the Ust'-Buotama outcrop.

In the Pre-Yakutsk geomorphological area, downstream of the Buotama-Sinsk, the Lena River valley is 200–280 km wide, and entrenched in terrigenous, predominantly sandy, Jurassic, Cretaceous, Paleogene and Neogene deposits. The Bestyakh Terrace occurs in the western part of the valley along the right bank of the river. It is inset in a Late Pliocene–Early Pleistocene terrace complex covered by Late Pleistocene deposits. The terrace extends for 120 km along the river, gradually widening northeastwards and lowering northwards. The maximum width (10–15 km) of the terrace occurs at the confluence of the Suola River where the surface elevation drops to 40–50 m above the modern channel (Nizhny Bestyakh outcrop). The terrace is 20–25 m above the modern channel (Peschanaya Gora outcrop) further downstream, in a 90-km segment of the valley terrace; however, this terrace is identified by some researchers as the Kerdem terrace (Ivanov, 1984; Kamaletdinov and Minuk, 1991). The surface of this terrace drops to 12–15 m above the modern channel near the Kharyalakh outcrop. Four units were distinguished in the terrace of the Pre-Yakutsk area, consisting of sediments of the Bestyakh, Mavrinka, Dolkuma Formations and Holocene deposits (Kamaletdinov and Minuk, 1991).

The Ust'-Buotama outcrop has been studied by a number of researchers. Alekseev et al. (1990) previously recognized three stratigraphic units in the section (from top to bottom): 1) aeolian sand correlated with the Upper Pleistocene; 2) lacustrine-alluvial sand deposited between the second half of the Middle Pleistocene and the beginning of the Late Pleistocene, with dating based on the remains of mammalian fauna (*Mammuthus* sp., *Coelodonta antiquitatis Blum.*, *Bison priscus Boj.*, *Ovis nivicola Esch.*, *Rangifer tarandus* L); and 3) alluvium of the Bestyakh Formation where two pollen assemblages were identified corresponding to the first half of the Middle Pleistocene. Kamaletdinov and Minuk (1991) also reported the occurrence of proluvial and slope-wash deposits, lying on the eroded alluvium of the Bestyakh Formation and overlain conformably by the Mavrinka Formation sediments. Based on the remains of mammalian fauna and radiometric data, this formation was constrained to MIS 8. The authors argued that the Mavrinka sediments were Middle Pleistocene periglacial alluvium rather than of lacustrine-alluvial origin. Pravkin et al. (2018) examined the stratigraphy of several exposures of the Bestyakh Terrace, including Ust'-Buotama. Eight metres below the terrace edge, they found interbeds of fine-to medium-grained, grayish-yellow quartz sand, showing massive cryostructure. Based on their geological and geomorphological study of key outcrops, the authors postulated a Late Pleistocene age for the Bestyakh Terrace.

3. Methods and measurement protocols

Here the Ust'-Buotama outcrop was reinvestigated using facies analysis and stratigraphic methods involving: geomorphological observations; identification, preparation and description of exposures; documentation of lithologic, sedimentary and cryostratigraphic structures; and sampling for radiocarbon and OSL dating. Several sections were prepared and explored in 2020 at the Ust'-Buotama site by a field team led by Professor A.A. Galanin using standard techniques including: excavation of multibench trenches from the terrace surface to water level; observations of sedimentary structures and facies; photographs and videos, and sampling for various analyses. Sedimentological analysis was based on modern understanding of mechanisms of aeolian and fluvial sedimentation in cold regions discussed in detail by Hunter (1977) and Galanin (2021).

Absolute dating of the deposits was performed using radiocarbon (7 samples) and luminescence methods (9 samples). Radiocarbon dating of three samples was completed at the Melnikov Permafrost Institute Radiocarbon Laboratory (Yakutsk) using liquid scintillation counting on the Quantulus 1220 spectrometer-radiometer. These three samples for radiocarbon dating were taken from Holocene aeolian dune: from palaeosol (PS-1) we selected buried pine trees with root system and humified wormwood; from palaeosol (PS-2) we took charcoal sample. Preparation of the samples for scintillation counting was carried out by sintering charcoal and lithium (lithium carbide), followed by additional hydrolyses and finally benzole synthesis by catalysis. For samples weighing less than 4 g and for disseminated carbon, benzole synthesis was performed using direct vacuum pyrolysis. ^{14}C-dating of additional four mollusc shell samples originating from the lacustrine-alluvial deposits were carried out in the AMS laboratory at the Institute for Nuclear Research, Debrecen, Hungary. Shell fragments were ultrasonically washed to remove surficial contaminations and carbonate mineral coatings were etched using weak acid (2% HCl). Subsequently, acid cleaned shell fragments were dried and dissolved by phosphoric acid. The resulting CO_2 was further purified cryogenically and then graphitized (Molnár et al., 2013a) before analysis using a compact radiocarbon AMS system (MICADAS; Molnár et al., 2013b). Radiocarbon age calibration used IntCal20 curve and OxCal 4.4 program (Reimer et al., 2020) at a 95% level of confidence.

Luminescence dating was performed using both optically stimulated luminescence (OSL) from quartz grains and infrared-stimulated luminescence (IRSL) from K-rich feldspar grains (Murray et al., 2021). Samples were collected from the central cleaned part of the outcrop (Fig. 2) from sandy and silty deposits. All samples were taken in opaque plastic tubes secured with foil at both ends and taped to retain moisture. Preliminary sample preparation was performed at the laboratory in Moscow under subdued orange LED lights (Sohbati et al., 2017). Quartz- and feldspar-rich extracts were obtained by wet sieving to 90–180 and 180–250 μm, followed by sequential treatment with 10% HCl, 10% H_2O_2 and 10% HF. Quartz and K-rich feldspar grains were then separated using a 2.58 g/cm^3 aqueous heavy liquid (potassium polytungstate) followed by additional purification of quartz in 40% HF (Murray et al., 2021).

Equivalent doses (D_e) were measured at the Nordic Laboratory for Luminescence Dating at Risø (DTU, Denmark) using a Risø TL/OSL DA-20 reader equipped with a calibrated beta source. For quartz, D_e was estimated using a single aliquot regenerative dose (SAR) protocol (Murray and Wintle, 2000, 2003), with 8-mm diameter aliquots mounted on stainless steel disks. Preheat was at 260 °C for 10 s, cut heat 220 °C for 10 s, and stimulation at 125 °C used blue (470 ± 30 μm) light for 40 s; photon detection was through 7-mm of U-340 glass filter. Finally, the aliquot was stimulated with blue light at 280 °C for 40 s at the end of each SAR cycle, to ensure that there was no remaining OSL signal. Before measurement of the equivalent dose, the absence of a

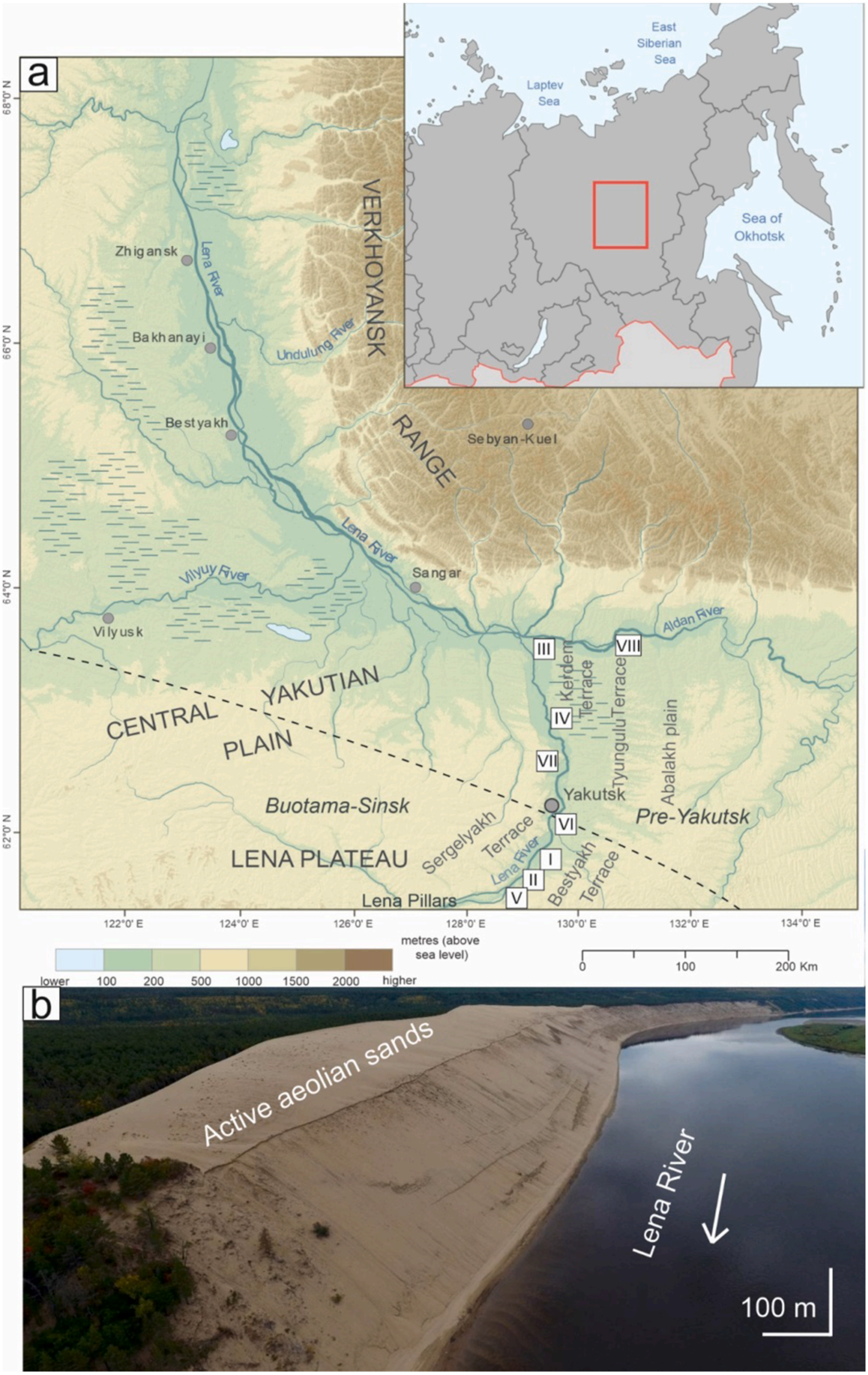

Fig. 1. a) The location and b) general view of the Ust'-Buotama outcrop: I) Ust'-Buotama outcrop; II) Diring Yuryakh site; III) Kharyalakh; IV) Peschanaya Gora; V) Saamys-Kumaga; VI) Nizhny Bestyakh; VII) Edeitsy; VIII) Mammoth Gora.

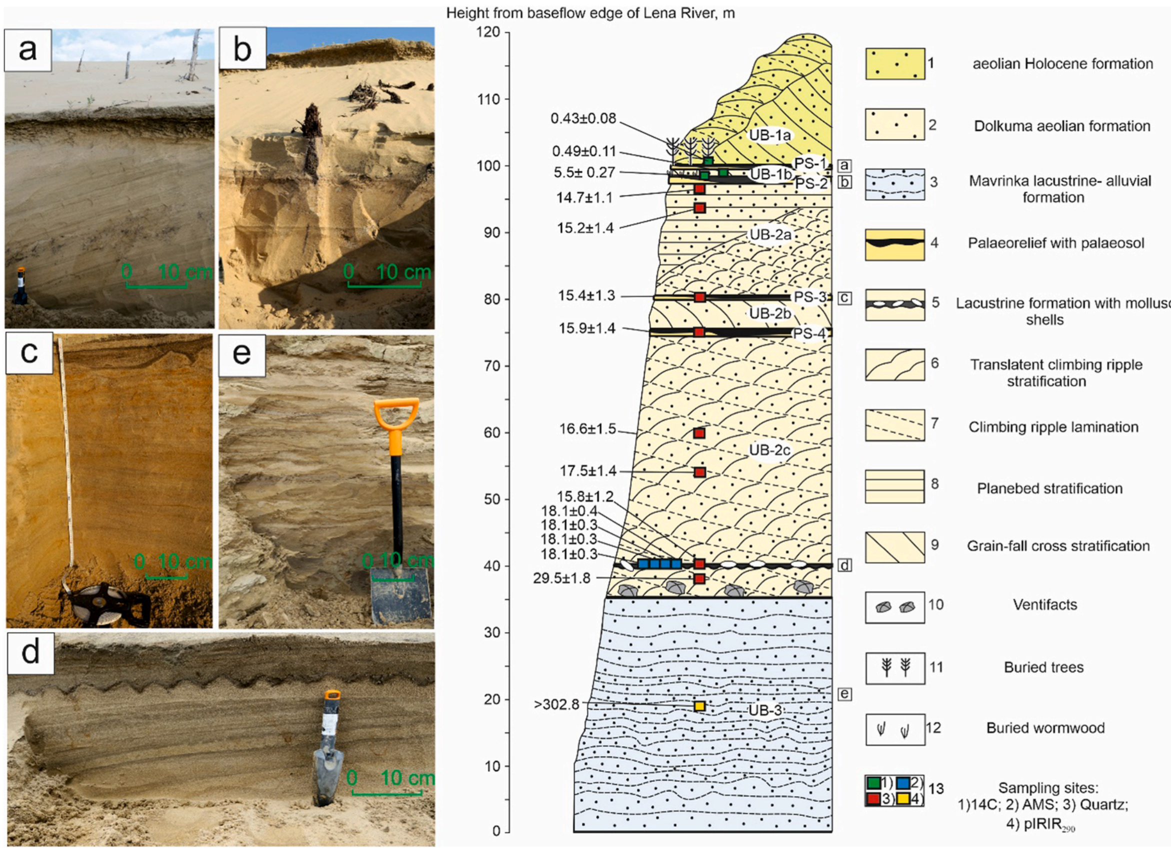

Fig. 2. Structure of the Ust'-Buotama section with preferred luminescence and radiocarbon ages in ka (see text): a) weakly developed palaeosol PS-1 with humus primers; b) palaeosol PS-2 with vertically buried tree trunk; c) palaeosol PS-3 with shallow vertical sandy pseudomorphs; d) remains of a buried lake in sandy deposits; e) Mavrinka Formation with wavy stratification.

significant IRSL signal from the quartz extracts was tested for, and samples that did not pass this test were treated once again with 40% HF and 10% HCl. Samples that still showed measurable IRSL signals after the additional etching step were measured with a double-SAR procedure by inserting an IR stimulation at 60 °C for 100 s in front of every blue light stimulation (Banerjee et al., 2001). Early background subtraction was used for D_e calculation - first 0.32 s minus a background from the subsequent 0.32 s of the decay curve (Cunningham and Wallinga, 2010).

For K-rich feldspar measurements we used 2-mm diameter aliquots mounted on stainless steel cups, and a post-IR IRSL SAR protocol (Thiel et al., 2011; Buylaert et al., 2012). Preheat following natural and regeneration doses was at a 320 °C for 60 s. Aliquots were then stimulated by IR light (850 ± 30 nm) for 200 s, first at 50 °C (IR_{50} signal) and then at 290 °C ($pIRIR_{290}$ signal). Late background (from the last 20s of stimulation) was subtracted from the first 2 s of the decay curve. We did not correct for any possible $pIRIR_{290}$ signal instability, following Thiel et al. (2011) and Buylaert et al. (2012). IRSL ages are used in age comparisons and discussion of the bleaching of the OSL signal from quartz before burial.

Measurements of the radionuclide concentrations were performed using high-resolution gamma spectrometry (Murray et al., 1987, 2018). Samples were first dried at 110 °C for 24 h, weighed and ignited at 450° for 24 h, before weighing again. The material was then ground, mixed with high viscosity wax and cast in a cup-shaped mould to provide a fixed counting geometry, and to prevent the loss of gaseous ^{222}Rn. After storing for >20 days to ensure ^{222}Rn equilibrium with its parent ^{226}Ra, samples were counted for 24 h. The resulting ^{226}Ra, ^{232}Th and ^{40}K activity were converted to dry infinite-matrix dose rates following Guerin et al. (2012), and assuming a 20 ± 10 % loss of ^{222}Rn under field conditions. For K-feldspar we assumed a K concentration of 12.5 ± 0.5% to calculate the internal beta dose rate (Huntley and Baril, 1997).

4. Results

4.1. *Stratigraphy of the Ust'-Buotama section*

We identify the following stratigraphic units (from top to bottom) in the central part of the Ust'-Buotama outcrop (Fig. 2).

I) Unit UB-1 (0–23 m)

Layer UB-1a (0–20 m): yellow fine-grained quartz sand; translatent climbing ripple stratification dipping southeast (155° azimuth) at a 30° angle. The laminae dip in the direction of aeolian transport and are parallel to each other. The top of UB-1 outcrops onto the surface as an unvegetated aeolian (Lena) dune. The lower boundary is smooth and clear.

Layer UB-1b (20–23 m): white to slightly yellowish fine-to medium-grained sand; inclined structure. The upper part of the layer consists of a weakly developed soil (PS-1) with numerous inclusions of charcoal; it is composed of thin interbeds of medium-grained sand and dark humified sandy loam; patches of humus are present which contain root systems of numerous vertically buried trees (pine) and humified wormwood (*Artemisia* sp.) roots, up to 5–6 cm in thickness. The lower part of the layer contains evidence of another palaeosol (PS-2) with frequent fragments of charcoal and occasional vertically buried dry pine trunks, up to 10–15 cm diameter. Palaeosol PS-2 consists of sandy loam and fine-grained sand, with inclusions of ochre-colored quartz sands and humus patches; the boundary is irregular, indistinct.

II) Unit UB-2 (23–85 m)

Layer UB-2a (23–40 m): white to slightly yellowish, fine-to medium-grained sand; plane bedded, subhorizontal stratification (Hunter, 1977).

Layer UB-2b (40–45 m): yellowish-grey, fine-to medium-grained sand with translatent climbing ripple stratification and climbing ripple lamination. The upper and lower boundaries are sharp, cut off by deflation surfaces. Palaeosol PS-3 at the top of layer UB-2b, 3–8 cm in thickness, is composed of thin-bedded sandy loam and fine-grained sand; plant residues are totally absent; cryogenic pseudomorphs are present. The complex geometry of the palaeosol is probably due to the differential movement of the base of the active layer during epigenetic freezing of sediments. Pseudomorphs resulted from cryoturbation in this weakly developed soil. Palaeosol PS-4 in the bottom of layer UB-2b was noticed during the reconnaissance survey; however, no signs of palaeosol were found after clearing the exposure.

Layer UB-2c (45–85 m): yellowish-white, fine-grained sand. Translatent climbing ripple stratification of the windward dune slope facies dipping southeast (130° azimuth) at 45° matches the dune orientation on the adjoining terrace and is opposite to the present flow of the Lena River. The structure is inclined. Evidence of a buried lake was found at a depth of 80–85 m as 3–5 cm thick dark-grey clays with mollusc shells. The bottom boundary of the layer is diffuse, irregular. The UB-2 deposits are here attributed to the Dolkuma Formation of Central Yakutia.

III) Unit UB-3 (85–120 m): thin-bedded sandy silty loam and sandy loam, dark-grey to blue-grey in color, showing evidence of gleying processes; wavy stratification; thin parallel, sometimes indistinct lamination. The bottom of the unit lies below the modern Lena River water level, while the top gradually plunges along the outcrop to the east from 35 to 10 m above the baseflow edge of the river. Interbeds of gravel and small pebbles of quartzite and limestone occur near the top of the layer, with some fragments showing signs of wind erosion (ventifacts). Unit UB-3 is here attributed to the Mavrinka Formation of Central Yakutia.

The alluvial sand and gravel deposits of the Bestyakh Formation are located below the Mavrinka Formation, but we were unable to study it because the top of the formation lies below the river's bank.

The stratigraphic units recognized in the Ust'-Buotama section suggest different origins for the sediments of the fourth terrace of the Lena River. The Bestyakh Formation consists of slightly ochreous gravel-pebble-sand deposits and is the basal alluvium of the Bestyakh Terrace. During field work, the top of the formation was below the modern riverbank, preventing us from studying it. Unit UB-3 lies on top of the Bestyakh Formation and is interpreted to contain floodplain lacustrine-alluvial deposits, which are attributed to the Mavrinka Formation, based on their structure and stratigraphic and geomorphological position; this formation is widespread in the region. The second unit, including layers UB-2a, UB-2b, UB-2c is interpreted as representing the Dolkuma Formation. Its characteristic feature is the presence of strata separated from each other by structural unconformities – deflation surfaces. Numerous features of the sedimentary layers indicate formation by wind of various directions and forces. The third UB-1 unit (UB-1a and UB-1b) is composed of Holocene aeolian cover.

4.2. Chronology

4.2.1. Dosimetry

The radionuclide activity concentrations and dry beta and gamma dose rate are presented in Table 1. The radionuclide concentrations ^{226}Ra, ^{232}Th and ^{40}K generally differ little from unit to unit; the activity concentration of ^{226}Ra is in the range 9–30 Bq.kg^{-1}, ^{232}Th 15–40 Bq.kg^{-1}. Sample 208225 contains the highest radionuclide activities (^{226}Ra – 30.7 ± 0.6 Bq.kg^{-1}, ^{232}Th – 41.4 ± 0.6 Bq.kg^{-1}). The content of ^{40}K within the outcrop is high and also varies only slightly by unit – 720–940 Bq.kg^{-1}. There is a high content of radionuclides in the base of the UB-2 unit, which is apparently due to the presence of pebbles and gravels in the layer.

Although ^{238}U concentrations are poorly constrained, the average activity ratio of ^{226}Ra/^{238}U is 1.03 ± 0.10 (n = 9) and we conclude there is no evidence for secular disequilibrium in the first part of the ^{238}U decay series; in the second half of the series, a ^{222}Rn escape of 20 ± 10% is assumed (Guerin et al., 2012).

Table 1
Radionuclide concentrations and dry infinite matrix beta and gamma dose rates.

Lab. code	H, m	^{238}U, Bq. kg^{-1}	^{226}Ra, Bq.kg^{-1}	^{232}Th, Bq.kg^{-1}	^{40}K, Bq. kg^{-1}	Beta dose rate, Gy. ka^{-1}	Gamma dose rate, Gy.ka^{-1}
208222	23	8 ± 5	11.8 ± 0.4	17.1 ± 0.4	801 ± 14	2.26 ± 0.04	0.92 ± 0.01
208223	25	19 ± 8	9.1 ± 0.6	17.0 ± 0.6	790 ± 15	2.20 ± 0.04	0.89 ± 0.01
218607	40	22 ± 5	18.1 ± 1.0	28.3 ± 0.8	884 ± 17	2.60 ± 0.05	1.16 ± 0.02
218608	45	14 ± 4	14.5 ± 0.6	18.4 ± 0.5	924 ± 12	2.60 ± 0.04	1.05 ± 0.02
218609	60	9 ± 4	12.3 ± 0.8	15.6 ± 0.6	843 ± 15	2.36 ± 0.04	0.93 ± 0.02
208226	66	13 ± 5	12.4 ± 0.5	17.0 ± 0.5	771 ± 15	2.19 ± 0.04	0.89 ± 0.02
218610	80	17 ± 5	17.6 ± 0.7	23.1 ± 0.6	935 ± 14	2.69 ± 0.04	1.13 ± 0.02
208225	82	27 ± 7	30.7 ± 0.6	41.4 ± 0.6	724 ± 15	2.42 ± 0.04	1.27 ± 0.03
208224	100	15 ± 8	15.3 ± 0.7	23.8 ± 0.7	786 ± 15	2.30 ± 0.04	1.01 ± 0.02

The main part of the outcrop is represented by sands with a low water content (with the exception of the lower layers, which served as zones of groundwater infiltration). The deposits contain pore ice, which forms massive and sublimation-contact cryostructures. All this indicates that since the formation of deposits of UB-1 and UB-2 units, the sands have remained in permafrost, so we selected a water content value of 25% for the sands. For the deposits of the UB-3 unit, due to the heavier texture and longer stay in the state of maximum moisture, we have selected a water content value equal to 40%. Total dose rates to quartz are given in Table 2; these do not vary significantly and range from 2.2 to 2.7 Gy ka^{-1}.

4.2.2. Quartz OSL characteristics

The quartz OSL signals are fast-component dominated and dose response curves are reproducible (Fig. 3a and b). The average dose recovery ratio (0.99 ± 0.05; n = 15) demonstrates that our chosen protocol can be used to reliably measure a known dose given before any heating of the sample; measured doses are plotted as a function of given doses in Fig. 3. The D_e estimates are also summarized in Table 2, together with the quartz OSL ages.

4.2.3. Feldspar luminescence characteristics

A typical K-rich feldspar $pIRIR_{50,290}$ dose response curve and IRSL curve (inset) are shown in Fig. 3c. Since these results are only used for testing whether quartz OSL signals were sufficiently bleached before deposition (Murray et al., 2012), no dose recovery tests or fading measurements have been undertaken. With the exception of the lowest two samples, the IRSL D_e estimates vary only slightly down the section (Table 2), from 51 to 59 Gy for the $pIRIR_{290}$ signal. Sample 208225 (82 m depth) gives a larger $pIRIR_{290}$ dose of 106.0 ± 1.7 Gy, and the deepest sample, 208225, is saturated, and has been assigned a $pIRIR_{290}$ dose of >1000 Gy. The ages resulting from these D_e estimates are also summarized in Table 2.

4.2.4. Radiocarbon and luminescence ages and bleaching

Both quartz OSL and $pIRIR_{290}$ ages vary over a similar range, from ~15 ka to ~30 ka. A comparison of the individual IRSL ages with OSL ages shows that in every case the IR_{50} ages are about 50% of the corresponding OSL age (Fig. 4, Table 2) and all $pIRIR_{290}$ ages are indistinguishable from the corresponding OSL age. Following the arguments of Murray et al. (2012) and Möller and Murray (2015) we identify those

Table 2
Quartz and K-feldspar luminescence dating results. Equivalent doses (D_e), total dose rates and ages.

Lab. code	H, m	Equivalent dose (Gy) and number of aliquots (n_r – rejected, n_a – accepted)									Total dose rate, Gy/ka		Age, ka			Feldspar/Quartz Age Ratios	
		Quartz OSL			$pIRIR_{290}$			IR_{50}					Quartz OSL	$pIRIR_{290}$	IR_{50}		
		D_e (Gy)	n_r	n_a	D_e (Gy)	n_r	n_a	D_e (Gy)	n_r	n_a	Quartz	Feldspar				IR_{50}/OSL	$pIRIR_{290}$/OSL
208222	23	33.6 ± 1.7	2	20	52.9 ± 1.0	1	5	22.9 ± 0.9	0	6	2.28 ± 0.11	3.23 ± 0.12	14.7 ± 1.1	16.4 ± 0.8	7.1 ± 0.4	0.48 ± 0.04	1.11 ± 0.10
208223	25	33.8 ± 2.5	0	20	51.9 ± 3.4	0	6	22.8 ± 1.3	0	6	2.22 ± 0.11	3.16 ± 0.12	15.2 ± 1.4	16.4 ± 1.3	7.2 ± 0.5	0.47 ± 0.05	1.08 ± 0.13
218607	40	41.5 ± 2.7	0	16	54.8 ± 0.7	1	7	26.3 ± 0.4	0	8	2.69 ± 0.13	3.64 ± 0.14	15.4 ± 1.3	15.1 ± 0.7	7.2 ± 0.3	0.47 ± 0.04	0.98 ± 0.09
218608	45	41.3 ± 2.9	0	16	59.9 ± 1.5	0	8	26.2 ± 0.9	1	7	2.60 ± 0.12	3.55 ± 0.14	15.9 ± 1.4	16.9 ± 0.9	7.4 ± 0.4	0.47 ± 0.05	1.06 ± 0.11
218609	60	38.9 ± 2.8	0	16	59.4 ± 2.1	1	7	29.7 ± 1.0	0	8	2.35 ± 0.11	3.29 ± 0.13	16.6 ± 1.5	18.0 ± 1.0	9.0 ± 0.5	0.54 ± 0.06	1.09 ± 0.11
208226	66	38.5 ± 2.3	1	19	54.8 ± 2.2	0	6	26.2 ± 0.7	0	6	2.20 ± 0.11	3.14 ± 0.12	17.5 ± 1.4	17.4 ± 1.0	8.4 ± 0.4	0.48 ± 0.04	1.00 ± 0.10
218610	80	43.0 ± 2.4	0	16	52.4 ± 2.1	0	8	28.1 ± 0.7	1	7	2.72 ± 0.13	3.67 ± 0.14	15.8 ± 1.2	14.3 ± 0.8	7.7 ± 0.4	0.49 ± 0.04	0.90 ± 0.09
208225	82	78.2 ± 2.5	1	17	105.5 ± 1.7	1	7	60.6 ± 4.0	1	7	2.65 ± 0.13	3.59 ± 0.14	29.5 ± 1.8	29.4 ± 1.4	16.9 ± 1.3	0.57 ± 0.06	0.99 ± 0.08
208224	100	>220	1	5	>1000	0	8	>400	2	6	2.36 ± 0.11	3.30 ± 0.13	>90	>300	>120	No data	

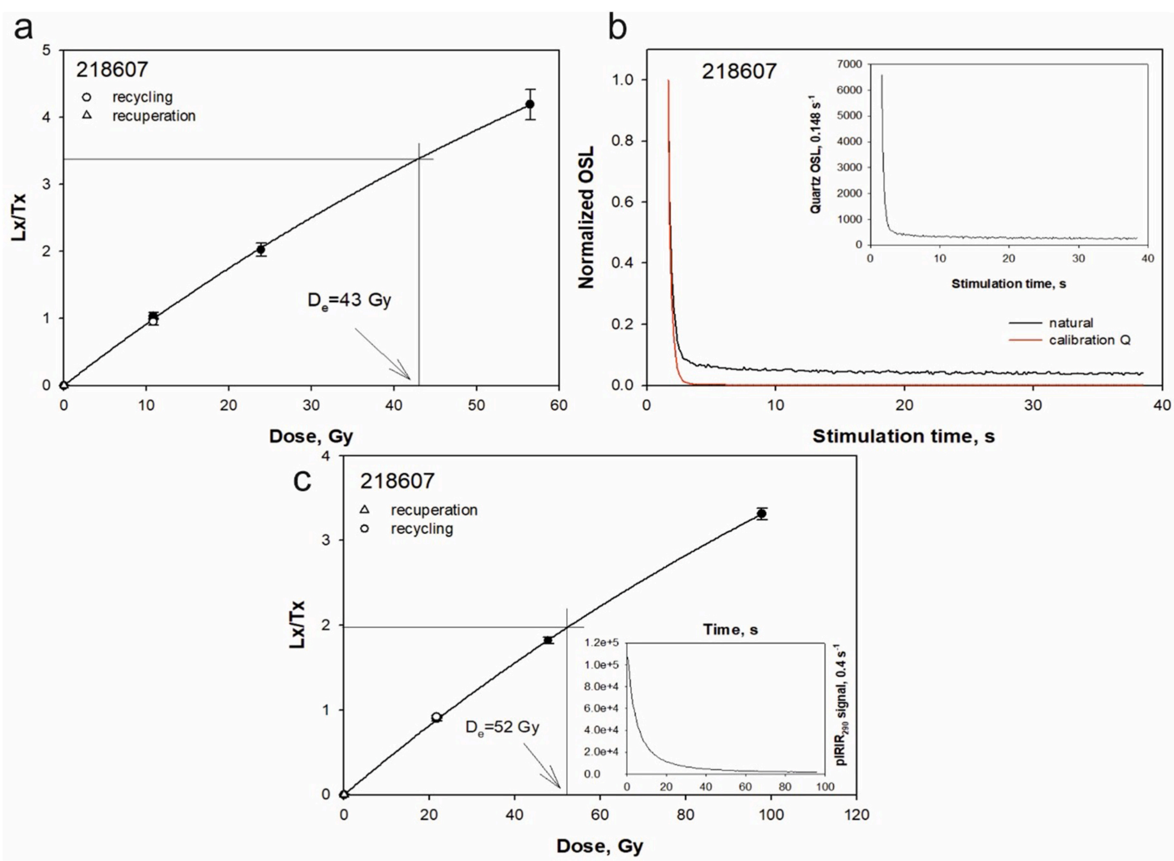

Fig. 3. Example luminescence characteristics for samples from Ust'-Buotama: a) Typical quartz OSL dose response curve; b) The natural OSL signal measured after IR stimulation at 60 °C compared with a decay curve from Risø calibration quartz; c) K-feldspar $pIRIR_{290}$ dose response curve for sample 218607 (inset shows the natural signal of an aliquot from this sample).

quartz OSL signals from samples which give IR_{50} ages less than or equal to OSL ages as 'probably sufficiently bleached' and those which give $pIRIR_{290}$ ages consistent with OSL ages as 'sufficiently bleached'. In our samples, all are 'sufficiently bleached', and so we consider our quartz OSL ages accurate, at least from the point of view of bleaching.

The ages from the section are all consistent with stratigraphic order. We only have independent age control for the lacustrine deposits and the youngest part of the outcrop. Radiocarbon measurements of four shell fragment samples collected from the lacustrine-alluvial deposits gave calibrated ^{14}C ages of 18.07 ± 0.35, 18.08 ± 0.34, 18.09 ± 0.31 and

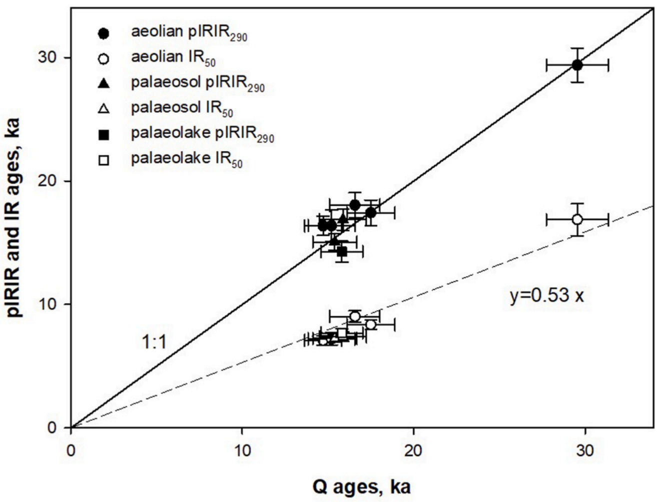

Fig. 4. $pIRIR_{290}$ and IR_{50} ages plotted against OSL ages.

18.10 ± 0.30 cal ka BP (Table 3).

Three radiocarbon ages were obtained for the upper part of the section, at the base of unit UB-1. In the bottom of layer UB-1b, fragments of palaeosol with charcoal were identified, from which we obtained a radiocarbon age of 5.50 ± 0.27 cal ka BP. The presence of a palaeosol indicates a period of stabilisation of the dune surface and aeolian sedimentation due to vegetation. The 'in situ' buried pine trees together with the root system from the top of layer UB-1b gave a ^{14}C age of 4.25 ± 0.80 cal ka BP, and 0.49 ± 0.11 cal ka BP for humified wormwood. We conclude that the formation of the top layer of UB-1b is associated with the last (modern) phase of aeolian activity occurring during the Little Ice Age.

Based on these results, we can now reconstruct the stages of the formation of the Ust'-Buotama section.

5. Discussion

Our new chronological data allow us to reconstruct, for the first time using absolute independent ages, the main stages of the middle Lena River evolution during the Middle and Late Pleistocene. We have established that the Bestyakh Terrace is not a fluvial terrace in the classic sense, but is rather the eroded remains of a complex deflation and accumulation plain. The terrace consists of 4 different stratigraphic formations: alluvial deposits of the Bestyakh Formation, lacustrine-alluvial deposits of the Mavrinka Formation, aeolian deposits of the Dolkuma Formation, and a modern Holocene (Lena) dune. The top of the Bestyakh Formation lies below river level, so we were unable to study these sediments. Thus, we identified 3 main units in the Ust'-Buotama outcrop; these reflect the major stages of sedimentation and development of the regional environment.

Table 3
Radiocarbon ages of mollusc shell fragments from the lacustrine deposits.

HEKAL code	pMC absolute	±1σ (abs)	conv.^{14}C age (ka BP)	±1σ (ka)	^{14}C age (cal ka BP)	±2σ
I/3674/1a	15.86	0.11	14.793	0.056	18.09	0.31
I/3674/1b	15.85	0.11	14.796	0.056	18.10	0.30
I/3674/1c	16.07	0.11	14.686	0.053	18.07	0.35
I/3674/1d	16.02	0.11	14.713	0.054	18.08	0.34

1. Unit UB-3 is represented by monotonous interbedding of sands, sandy loams and loams with a rare inclusion of gravel and small pebbles of quartzite and limestone. The structure and stratigraphic position of the unit allow us to confidently correlate it with the classic Mavrinka Formation of Central Yakutia, the origin and age of which are still debated. Initially, the genesis of the deposits was determined as lacustrine-alluvial, and the age as lying between MIS 7 and MIS 5 (Kolpakov, 1983). Kamaletdinov and Minuk (1991) determined its age as between MIS 7 and MIS 6, based on isolated single palinospectres in the sediments. We believe that the characteristics of the deposits of the Mavrinka Formation fully correspond to the widely developed Middle Pleistocene periglacial alluvium in European Russia. It is assumed that the Formation resulted from the build-up of a glacially-dammed lake by the presumed blocking of the Lena River by the Verkhoyansk glaciers (Kolpakov, 1966, 1983). The possible blocking of the riverbed by the glacier is indicated by the findings of Verkhoyansk moraines with interlayers of ventifacts overlain by dune and ice-loess deposits on the left bank of the Lena River. In the part of the Ust'-Buotama section examined here, the characteristics of the formation also indicate lacustrine-alluvial genesis. A more detailed reconstruction of the genesis of the Mavrinka Formation is required to allow us to determine whether it formed in an extensive glacially-dammed lake or rather subaerially on the floodplain in the Lena River valley. In any case, the minimum age of >300 ka suggests that this unit belongs to MIS 9 or older, considerably older than previously suggested. Possible glacial-dammed lake deposition does not invalidate this conclusion, because the sediments would have been delivered to the lake basin by the Lena River, and so would likely have experienced bleaching in an alluvial and fluvial environment before and during transport as previously shown for larger rivers in Northern Eurasia (Utkina et al., 2022; Kurbanov et al., 2021; Mangerud et al., 2004). The age obtained for the Mavrinka Formation indicates that age of the Bestyakh Terrace is older than 300 ka. The surface of the Mavrinka Formation (UB-3) is denuded and the aeolian deposits of unit UB-2 overly it unconformably. Based on our new ages, this unconformity represents a significant hiatus lasting at least 300 ka, presumably arising from intensive aeolian processes and significant deflation of the underlying Mavrinka Formation, as indicated by ventifacts found at the base of unit UB-2.
2) Unit UB-2 formed under subaerial conditions in the cold and dry environment of the Late Pleistocene. Based on the analysis of sedimentary structures, we identify several layers within the unit – layers UB-2c, UB-2b and UB-2a, identified as the Dolkuma Formation. These layers are made up of well-sorted light sands with a thickness of up to 65 m. Structural features and the nature of the layering indicate that each layer represents a fossil dune.

Our new chronology suggests that the accumulation of these 65 m of dune deposits began at the end of MIS 3 and continued intermittently in MIS 2. At the bottom of the UB-2c unit at depths of 82 and 80 m from the top of the dune, we obtained OSL ages of 29.5 ± 1.8 ka (208225) and 15.8 ± 1.2 ka (218610), respectively. This suggests a significant discontinuity in sedimentation representing about 14 ka. This discontinuity is probably associated with the appearance of a small buried lake with mollusc shells found in the sediments. Radiocarbon ages of the mollusc shell fragments (~18.1 ± 0.3 ka) further confirm this chronology (Table 3).

It is possible that at the end of MIS 3, regional conditions were wetter and warmer for some time; this would have contributed to ponding in the inter-dune depressions and to wider vegetation development, all contributing to a sharp decrease in the intensity of aeolian processes. Our results are consistent with earlier interpretations of the Dolkuma Formation (Kamaletdinov and Minuk, 1991; Pravkin et al., 2018). The deposition of this formation involved extensive aeolian processes and cryogenesis. This led to the formation of a large variety of mixed cryogenic-aeolian, niveo-aeolian, aeolian-fluvial and aeolian-lacustrine facies. Several periods of stabilisation of the aeolian relief are noted in the upper part of the Dolkuma Formation within the Ust'-Buotama outcrop; these are expressed in UB-2b and UB-2a as several weakly developed palaeosols (PS-3 and PS-4). These periods of stabilisation indicate that at the end of MIS 2 there were phases of decreased aeolian activity and periods of short-term fixation of dunes with herbaceous vegetation around 16-15 ka. These palaeosols were affected by cryogenic phenomena, expressed in the form of small pseudomorphs.

3. Unit UB-1 is represented by aeolian sands with characteristic structure types. The top of the unit is exposed at the surface in the form of an unstabilised Lena Dune. Based on our new radiocarbon ages, the formation of the unit is associated with the last (recent) phase of activation of aeolian processes, which the age suggests occurred during the Little Ice Age (about 1300–1850 CE). Many modern dune massifs within Central Yakutia are of similar age (Kut, 2015). The radiocarbon age obtained from underlying unit UB-1b (5.5 ± 0.27 cal ka BP) occurs close to the end of Holocene 'optimum' conditions in the early to middle Holocene (Kaufman and Broadman, 2023), and thus could indicate Neoglacial climate deterioration-driven dune reactivation, after relative stability under warmer, wetter early to mid-Holocene conditions.

In addition to extensive sand cover in Central Yakutia, there is also a widely distributed thick ice-rich silts with syngenetic ice wedges, known as the Yedoma Formation, Ice Complex or Loess-Ice Formation (Geocryology of the USSR, 1989). Yedoma covers most of the North-Eastern Siberia 1000–2000 km north-east from Lena River valley. It is believed that the ice-loess deposits of Yedoma Formation are the products of the reworking of the Quaternary alluvium of the Lena River (Pewe and Journaux, 1983), which also formed the sand cover in Central Yakutia (Dolkuma Formation). Our new understanding of the chronology of the Dolkuma Formation is in good agreement with the suggested age of much of the Yedoma (MIS 3) (Wetterich et al., 2014), but the precise chronostratigraphic relationships between dune activity and Yedoma formation require detailed sampling of both.

6. Conclusion

Here we present new results from a detailed study of the structure of the Ust'-Buotama outcrop, part of the Bestyakh Terrace of the Lena River. Except for the Mavrinka Formation, much of the terrace sediment appears to have been deposited under subaerial conditions in the cold, dry environments of the Late Pleistocene. The new chronology developed here allows us to draw the following conclusions:

Four heterogeneous units contribute to the structure of the Quaternary deposits in the Ust'-Buotama outcrop.

(a) Alluvial sand-gravel ochreous deposits with an admixture of pebbles (Bestyakh Formation). The formation lies below the river's edge, and at present there are no absolute ages for this deposit.

(b) The UB-3 unit (85–120 m depth from the top) correlates with the deposits of the Mavrinka Formation. Our $pIRIR_{290}$ ages indicate for the first time that the formation is at least 300 ka old (MIS 9 or older) and the age of the Bestyakh Terrace is older than 300 ka. According to the classical concept, these lacustrine and lacustrine-alluvial loams and sandy loams accumulated in a proglacial lake, dammed by a glacier that descended from the western slope of the Verkhoyansky ridge.

(c) Unit UB-2 (23–85 m depth from the top) reflects various periods of dominant aeolian processes in Central Yakutia. Sedimentological descriptions indicate a series of superimposed fossil dunes and periods of deflation. Our new OSL and ^{14}C ages from UB-2 (ranging from 29.5 ka to 14.7 ka) indicate that this unit formed between the end of MIS 3 and the late MIS 2, during two phases; taken together with the observed structural characteristics, we attribute this unit to the Dolkuma Formation. At the end of Last Glacial Maximum (21-18 ka), aeolian relief formation reached its widest extent in Central Yakutia. Residual alluvial, lacustrine and glacial deposits all underwent aeolian reworking. This event is associated with the maximum extent of sand dune massifs and cover, and stone ventifact deserts in Central Yakutia.

(d) Unit UB-1 indicates Late Holocene dunes activity, the surface of which is active today. Based on a single radiocarbon age (5.50 ± 0.27 cal ka BP) the unit began to form during Neoglacial cooling at the end of the Holocene optimum. Radiocarbon ages obtained from the upper part of the unit (ages of 400 cal a BP) indicate Late Holocene dune formation associated with cooling and desiccation of the climate during the Little Ice Age (1300–1850 CE). Many currently active dune massifs in Central Yakutia have similar ages (Kut, 2015).

These first results of luminescence dating of the Lena River terraces show the great potential of this method for developing of a reliable chronology of the palaeogeographic history of the region and in constraining the evolution of the river valley. For the first time we provided absolute ages for the Mavrinka Formation of Central Yakutia and evidence of a long mid to late Pleistocene hiatus and several late Pleistocene deflation events. Dating of the Ust'-Buotama reference section has also allowed reconstruction of the complicated history of the aeolian landscapes, widespread in the region in the second half of the Late Quaternary. Future studies should provide a better understanding of the age and sedimentation history for the Mavrinka Formation and the evolution of the sand seas of Central Yakutia – a possible large source of sediments for the loess-Yedoma accumulation in North-Western Siberia.

CRediT authorship contribution statement

Anzhela N. Vasilieva: Writing – original draft, Resources, Formal analysis, Data curation. **Andrew S. Murray:** Writing – original draft, Visualization, Software, Methodology, Formal analysis. **Natalia A. Taratunina:** Visualization, Methodology, Formal analysis. **Jan-Pieter Buylaert:** Writing – original draft, Visualization, Software, Methodology, Conceptualization. **Vasiliy M. Lytkin:** Data curation, Conceptualization. **Grigoriy I. Shaposhnikov:** Formal analysis, Data curation. **Thomas Stevens:** Writing – original draft, Visualization, Formal analysis, Conceptualization. **Gábor Ujvari:** Writing – original draft, Visualization, Methodology, Formal analysis, Data curation, Conceptualization. **Titanilla G. Kertész:** Methodology, Formal analysis. **Redzhep N. Kurbanov:** Writing – original draft, Visualization, Methodology, Formal analysis, Data curation, Conceptualization.

Declaration of competing interest

The authors declare that they have no known competing financial interests or personal relationships that could have appeared to influence the work reported in this paper.

Data availability

Data will be made available on request.

Acknowledgements

This paper is dedicated to the loving memory of our colleague, teacher and friend Alexey Galanin (February 25, 1969–September 08, 2022), whose energy and active work started new stage in study of palaeogeography and geomorphology of Northeast Asia.

This study was supported by project № 21-17-00054 (Quaternary aeolian relief and cover deposits of Lena River basin (Eastern Siberia):

structure, age and paleoenvironment significance). Radiocarbon samples were carried out as part of the project № 122011800064-9 «The structure and key stages of the evolution of the continental cryolithozone in the Neopleistocene and Holocene».

References

Alekseev, M.N., 1978. Anthropogenic of East Asia: Stratigraphy and Correlation. Nauka, Moscow, p. 205 (In Russ.).
Alekseev, M.N., Kamaletdinov, V.A., Grinenko, O.V., 1984. Cenozoic deposits of the Lena and Aldan. In: 27th International Geological Congress. Yakut ASSR, Siberian Platform. Generalized Guide of Excursions 052, 053, 054, 055. Nauka, Novosibirsk, pp. 21–42 (In Russ. and in Eng.).
Alekseev, M.N., Grinenko, O.V., Kamaletdinov, V.A., et al., 1990. Neogenovye i chetvertichnye otlozheniya nizhnealdanskoj vpadiny i srednej leny (Central'naya Yakutiya) [Neogene and Quaternary Deposits of the Lower Aldan Depression and the Middle Lena (Central Yakutia)]. Geological excursion guide. Yakutsk, YaNC SO AN SSSR 42 (In Russ.).
Banerjee, D., Murray, A.S., Bøtter-Jensen, L., Lang, A., 2001. Equivalent dose estimation using a single aliquot of polymineral fine grains. Radiat. Meas. 33 (1), 73–94.
Buylaert, J.-P., Jain, M., Murray, A.S., Thomsen, K.J., Thiel, C., Sohbati, R., 2012. A robust feldspar luminescence dating method for Middle and Late Pleistocene sediments. Boreas 41, 435–451. https://doi.org/10.1111/j.1502-3885.2012.00248.x.
Cunningham, Alastair C., Jakob, Wallinga, 2010. Selection of integration time intervals for quartz OSL decay curves. Quat. Geochronol. 5 (6), 657–666. https://doi.org/10.1016/j.quageo.2010.08.004.
Galanin, A.A., 2021. Late Quaternary sand covers of Central Yakutia (Eastern Siberia): Structure, facies composition and paleoenvironment significance. Kriosfera Zemli 25, 3–34. https://doi.org/10.15372/KZ20210101 (In Russ.).
Galanin, A.A., Pavlova, M.R., 2019. Late Quaternary dune formations (D'olkuminskaya Series) in Central Yakutia (Part 2). Kriosfera Zemli [Earth's Cryosphere] XXIII (1), 3–15 (In Russ.).
Galanin, A.A., Pavlova, M.R., Klimova, I.V., 2018. Late Quaternary dune formations (D'olkuminskaya Series) in Central Yakutia (Part 1). Kriosfera Zemli [Earth's Cryosphere] XXII (6), 3–14 (In Russ.).
Geocryology USSR, 1989. In: Ershov, E.D. (Ed.), Srednyaya Sibir [Geocryology of USSR. Middle Siberia]. Nedra, Moscow, p. 414 (In Russ.).
Geology of the USSR, 1979. Volume XVIII. The western part of the Yakut ASSR. Part. 1. In: Markov, F.G. (Ed.), Geological Description. Book 1. M.: Publishing house "Nedra", p. 535 (In Russ.).
Grinenko, V.S., Kamaletdinov, V.A., Slastenov, Yu L., Scherbakov, O.I., 1995. The geological structure of Yakutsk//Regional geology of Yakutia: collection of scientific articles. Yakutsk. publishing house of YSU, p. 155 (In Russ.).
Guerin, G., Mercier, N., Nathan, R., Adamiec, G., Lefrais, Y., 2012. On the use of the infinite matrix assumption and associated concepts: a critical review. Radiat. Meas. 47, 778–785. https://doi.org/10.1016/j.radmeas.2012.04.004.
Hunter, R.E., 1977. Basic types of stratification in small eolian dunes. Sedimentology 24, 361–387. https://doi.org/10.1111/j.1365-3091.1977.tb00128.x.
Huntley, D.J., Baril, M.R., 1997. The K content of the K-feldspars being measured in optical dating or in thermoluminescence dating. Ancient TL 8, 2–13.
Ivanov, M.S., 1984. Kriogennoe Stroenie Chetvertichnyh Otlozhenij Leno-Aldanskoj Vpadiny [Cryogenic Structure of the Quaternary Deposits of the Lena-Aldan Depression]. Nauka, Novosibirsk, p. 126 (In Russ.).
Kamaletdinov, V.A., Minuk, P.S., 1991. Structure and characteristics of sediments of the bestyakh terrace of the middle Lena River. Byulleten' Komissii po izucheniyu chetvertichnogo perioda AN SSSR [Bulletin of the Commission of Quaternary Research of AS USSR] (60), 68–78 (In Russ.).
Katasonov, E.M., Ivanov, M.S., 1973. Kriolitologiia Tsentral'noi Iakutii (ekskursiia po Lene i Aldanu): Putevoditel' [Cryolithology of Central Yakutia (excursion on Lena and Aldan): Guide]. Izd. OUPES SO AN SSSR, Iakutsk (In Russ.), 1-37.
Kaufman, D.S., Broadman, E., 2023. Revisiting the Holocene global temperature conundrum. Nature 614, 425–435. https://doi.org/10.1038/s41586-022-05536-w.
Kolpakov, V.V., 1966. Palaeogeography of the Quaternary period in the lower reaches of the Lena River//Izv. vuzov. Ser. geol. i razv. 5, 41–48 (In Russ.).
Kolpakov, V.V., 1983. Aeolian Quaternary deposits in the Lena area of Yakutia. Bulletin of the Commission of Quaternary Research (Billyuten po izuchen. chetvert. perioda) 52, 123–131 (In Russ.).
Korzhuev, S.S., 1977. Geomorphology of the Middle Lena Valley and Surrounding Areas. Izdatel'stvo AN SSSR, Moskva, p. 152 (In Russ.).
Kurbanov, R., Murray, A., Thompson, W., et al., 2021. First reliable chronology for the early Khvalynian Caspian Sea transgression in the Lower Volga River valley. Boreas 50 (1), 134–146. https://doi.org/10.1111/bor.12478.
Kut, A.A., 2015. Aeolian-permafrost dune massifs (tukulans) in Central Yakutia: their structure, genesis, age and distribution patterns. Extended abstract of Cand. Sci. (geol.-mineral.) Dissertation. Yakutsk 22 (In Russ.).
Lukyanycheva, M., Kurbanov, R., Taratunina, N., Vasilieva, A., Lytkin, V., Panin, A., Anoikin, A., Stevens, T., Murray, A., Buylaert, J.-P., Knudsen, M., 2024. Dating post LGM aeolian sedimentation and the Late Palaeolithic in Central Yakutia (Northeastern Siberia). Quat. Geochronology, V. 83, 2024, 101563. https://doi.org/10.1016/j.quageo.2024.101563.
Lungersgauzen, G.F., 1957. Stratigraphy of Quaternary sediments of the eastern part of the Siberian platform. Proceedings of the Interdepartmental Meeting on the Development of Unified Stratigraphic Schemes of Siberia. Gostoptechizdat (In Russ.).
Lungersgauzen, G.F., 1961. Stratigraphy of Cenozoic Deposits of the Middle and Lower Lena and its Delta//Meeting on the Development of Stratigraphic Schemes of the Yakut ASSR: Tez. Dokl. L, pp. 178–182 (In Russ.).
Mangerud, J., Jacobsson, M., Alexanderson, H., Astakhov, V., Clark, G.K., Henriksen, M., Hjort, C., Krinner, G., Lunnka, J.P., Möller, P., Murray, A., Nikolskaya, O., Saarnisto, M., Svendsen, J.I., 2004. Ice-dammed lakes and rerouting of the drainage of northern Eurasia during the Last Glaciation. Quat. Sci. Rev. 23 (11–13), 1313–1332. https://doi.org/10.1016/j.quascirev.2003.12.009, 2004.
Möller, P., Murray, A.S., 2015. Drumlinised glaciofluvial and glaciolacustrine sediments on the Småland peneplain, South Sweden–new information on the growth and decay history of the Fennoscandian Ice Sheets during MIS 3. Quat. Sci. Rev. 122, 1–29.
Molnár, M., Janovics, R., Major, I., Orsovszki, J., Gönczi, R., Veres, M., Leonard, A.G., Castle, S.M., Lange, T.E., Wacker, L., Hajdas, I., Jull, A.J.T., 2013a. Status report of the new AMS ^{14}C sample preparation lab of the hertelendy laboratory of environmental studies (Debrecen, Hungary). Radiocarbon 55, 665–676.
Molnár, M., Rinyu, L., Veres, M., Seiler, M., Wacker, L., Synal, H.-A., 2013b. ENVIRONMICADAS: a mini 14C AMS with enhanced gas ion source interface in the Hertelendi Laboratory of Environmental Studies (HEKAL). Hung. Radiocarbon 55, 338–344.
Murray, A.S., Wintle, A.G., 2000. Luminescence dating of quartz using an improved single-aliquot regenerative-dose protocol. Radiat. Meas. 32 (1), 57–73. https://doi.org/10.1016/S1350-4487(99)00253-X.
Murray, A.S., Wintle, A.G., 2003. The single aliquot regenerative dose protocol: potential for improvements in reliability. Radiat. Meas. 37, 377–381.
Murray, A.S., Marten, R., Johnston, A., Martin, P., 1987. Analysis for naturally occurring radionuclides at environmental concentrations by gamma spectrometry. J. Radioanal. Nucl. Chem. 115, 263–288.
Murray, A.S., Thomsen, K.J., Masuda, N., et al., 2012. Identifying well-bleached quartz using the different bleaching rates of quartz and feldspar luminescence signals. Radiat. Meas. 47, 688–695.
Murray, A.S., Helsted, L.M., Autzen, M., Jain, M., Buylaert, J.-P., 2018. Measurement of natural radioactivity: calibration and performance of a high-resolution gamma spectrometry facility. Radiat. Meas. 120, 215–220. https://doi.org/10.1016/j.radmeas.2018.04.006.
Murray, A., Arnold, L.J., Buylaert, J.-P., Guérin, G., Qin, J., Singhvi, A.K., Smedley, R., Thomsen, K.J., 2021. Optically stimulated luminescence dating using quartz. Nature Reviews Methods Primers 1 (72). https://doi.org/10.1038/s43586-021-00068-5.
Pewe, T.L., Journaux, A., 1983. Origin and character of loess-like silt in unglaciated south-central Yakutia. Siberia, U.S.S.R. Geological Survey. United States Government Printing Office, Washington, p. 46. Professional paper 1262.
Pravkin, S.A., Bolshiyanov, D.Yu, Pomortsev, O.A., et al., 2018. Relief, structure and age of Quaternary sediments of the river valley. Lena in the Yakutsk bend. Vestnik Sankt-Peterburgskogo universiteta. Nauki o Zemle [Bulletin of St. Petersburg University. Earth Sciences 63 (2), 209–229 (In Russ.).
Reimer, P., Austin, W., Bard, E., Bayliss, A., Blackwell, P., Bronk Ramsey, C., Talamo, S., 2020. The IntCal20 Northern Hemisphere Radiocarbon Age Calibration Curve (0-55 cal kBP). Radiocarbon 62 (4), 725–757. https://doi.org/10.1017/RDC.2020.41.
Rusanov, B.S., 1968. Biostratigraphy of Cenozoic Deposits of South Yakutia. Nauka Publishing House (In Russ.).
Sohbati, R., Murray, A., Lindvold, L., Buylaert, J.-P., Jain, M., 2017. Optimization of laboratory illumination in optical dating. Quat. Geochronol. 39, 105–111.
Soloviev, P.A., 1959. Kriolitozona Severnoj Chasti Leno-Amginskogo Mezhdurech'ya [Cryolithozone of the Northern Part of the Lena-Amga Interfluve. AN SSSR, Moscow, p. 144 (In Russ.).
Spektor, V.B., Spektor, V.V., 2002. O proiskhozhdenii vysokoi Leno-Amginskoi perigliatsial'noi ravniny [On genesis of high Lena-Amga rivers periglacial plain]. Kriosfera Zemli VI, 4, 3–12. (In Russ.).
Thiel, C., Buylaert, J.-P., Murray, A., Terhorst, B., Hofer, I., Tsukamoto, S., Frechen, M., 2011. Luminescence dating of the Stratzing loess profile (Austria) – testing the potential of an elevated temperature post-IR IRSL protocol. Quat. Int. 234, 23–31. https://doi.org/10.1016/j.quaint.2010.05.018.
Utkina, A.O., Panin, A.V., Kurbanov, R.N., Murray, A.S., 2022. Unexpectedly old luminescence ages as an indicator of the origin of the upper Volga River valley sediments. Quat. Geochronol. 73M, 101281 https://doi.org/10.1016/j.quageo.2022.101381.
Waters, M.R., Forman, S.L., Pierson, J.M., 1997. Diring Yuriakh: A Lower Paleolithic site in central Siberia. Science 275, 1281–1284. https://doi.org/10.1126/science.275.5304.1281.
Waters, M.R., Forman, S.L., Pierson, J.M., 1999. Late Quaternary geology and geochronology of Diring Yuriakh, an early paleolithic site in central Siberia. Quat. Res. 51 (2), 195–211.
Wetterich, S., Tumskoy, V., Rudaya, N., Andreev, A., Opel, T., Meyer, H., Schirrmeister, L., Hüls, M., 2014. Ice complex formation in arctic East Siberia during the MIS3 interstadial. Quat. Sci. Rev. 84, 39–55.
Zol'nikov, V.G., Popova, A.I., 1957. Paleogeograficheskaia skhema chetvertichnogo perioda ravniny Tsentral'noi Iakutii [Paleogeographic scheme of the Quaternary of the plain of Central Yakutia]. Tr. Inst. Biol. 3, 5–8 (In Russ.).